ROBUST SILICON CARBIDE (SiC) NANOELECTROMECHANICAL SWITCHES WITH LONG CYCLES IN AMBIENT AND HIGH TEMPERATURE CONDITIONS

Tina He[1†], *Rui Yang*[1], *Srihari Rajgopal*[1], *Mary Anne Tupta*[2],
Swarup Bhunia[1], *Mehran Mehregany*[1†], *and Philip X.-L. Feng*[1†]
[1]Electrical Engineering, Case Western Reserve University, Cleveland, OH 44106, USA
[2]Keithley Instruments, Inc., Cleveland, OH 44139, USA
[†]Email: ting.he@case.edu; mehran@case.edu; philip.feng@case.edu

ABSTRACT

We report experimental demonstration of nanoscale electromechanical contact-mode switches with clearly high comparative performance, enabled by polycrystalline silicon carbide (poly-SiC) nanomechanical cantilevers, in a three-terminal, gate-controlled, lateral configuration. We have recorded the complete time evolution of the measured switching events in ambient air, by switching devices on and off for $\geq 10^5$–10^6 cycles without failure (*i.e.*, devices still alive; special accelerated tests are needed to properly 'exhaust' the device and approach its intrinsic lifetime). These SiC nanoelectromechanical systems (NEMS) based switches have all dimensions but length in nanometer scale, and demonstrate on/off ratios of ~10^4 or higher, with repeatable performance over days in air. We have also demonstrated SiC NEMS switches operating at high temperature ($T \approx 500$°C) in air. With a typical motional volume of only ~1μm^3 and long 'hot' switching cycles in air, these SiC devices exhibit strong potential toward realizing robust NEMS switches and logic circuits.

INTRODUCTION

Contact-mode MEMS/NEMS logic switches (relays) have been rapidly emerging, and have been actively explored as a promising candidate for ultralow-power applications [1-5]. Truly miniaturized and scaled, NEMS switches can offer compelling attributes and comparative advantages including ideally abrupt switching with minimal off-state leakage, suitable for high temperature and extreme environments, and small footprints. In this pursuit, however, major challenges remain: (i) all recently reported high-performance mechanical switches are still very much in the MEMS domain [2-5] and are orders of magnitude larger in size/volume than today's mainstream transistors. In fact, recent MEMS switches with excellent cycle numbers [3-5] are all $\geq 10^3$ to $\geq 10^4$ times larger in *motional volume* than NEMS devices reported in this work. (ii) Most of today's truly nanoscale mechanical switches, however, suffer from very short lifetime, and some can merely switch one or a few cycles before failure [6-11].

We report here very small lateral electrostatic NEMS performing contact-mode 'hot' switching in air, at ~25°C and 500°C, using gate-coupled nanocantilevers made of poly-SiC, which is uniquely suited for NEMS for its outstanding mechanical, chemical and thermal properties. Switching events and long cycles of actuation recorded in real time suggest that high on/off ratios (>10^4) and long lifetime are achievable in SiC NEMS (both in air and in harsh environments) that have very small contact areas (~0.01–0.1μm^2) and motional volumes (~1μm^3).

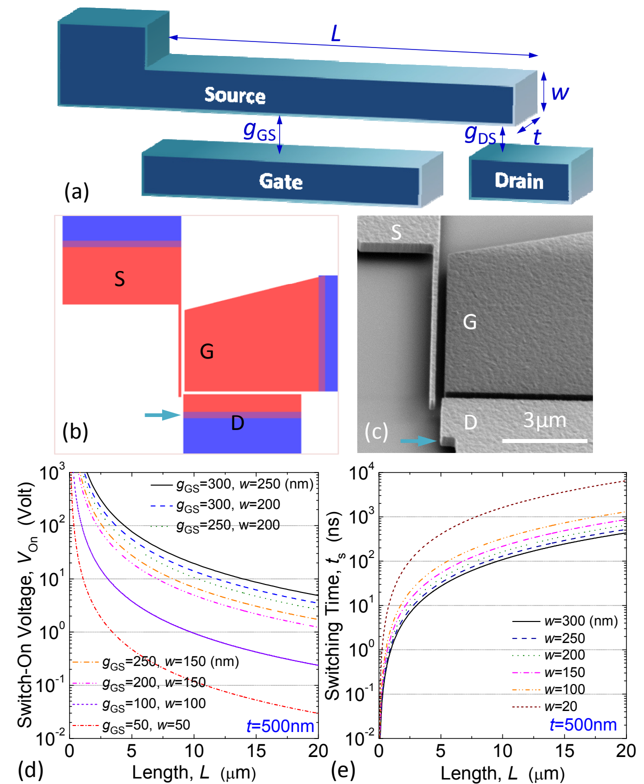

Figure 1: Lateral SiC electrostatic NEMS switch design and analytical modeling. (a) 3D illustration of device with key geometric parameters. (b) Layout of a typical device. Red & blue denote regions to be patterned using different parameters in electron-beam lithography (EBL). (c) SEM image of a fabricated device shown in (b). The notch (arrows in (b) & (c)) is due to change in EBL settings. (d) & (e) Modeling results for design with tradeoffs, showing switch-on voltage and switching time dependency on device geometry and dimensions (for a 500nm SiC film).

DESIGN AND FABRICATION

Figure 1a illustrates the gate-controlled electrostatic nanocantilever for realizing three-terminal lateral NEMS switches. Most devices have thicknesses, widths, and gaps ~200–300nm or smaller. Figure 1b & c show an example of a specific design pattern and the actual device's image. A voltage (V_G) applied on the gate (G) electrostatically actuates the cantilever, which is the movable source (S), grounded at its clamping port. We design the devices so that the cantilever deflection is controlled by electrostatic coupling from the gate – when V_G is just above a certain threshold V_{on}, the cantilever tip makes contact ('switch') to the drain (D) which is gently biased (often $V_D \ll V_G$), thus allowing a drain current I_D to pass from D to S. As long as

fabrication is possible with acceptable yield, smallest g_{GS} and g_{DS} are both desired for lowering V_{on} and decreasing switching time t_s. To attain abrupt switching at $V_G \geq V_{on}$, approximately $g_{GS} > g_{DS} \geq g_{GS}/3$ is also desired. In this case, by using a lumped-parameter model, we estimate that the 'switching-on' or threshold voltage should be

$$V_{on} \approx \left(8k_{eff} g_{GS}^3 / 27\varepsilon_0 t L_G\right)^{1/2}, \quad (1)$$

and at $V_G = V_{on}$, the switching time is approximately

$$t_s \approx \sqrt{27/2} / \omega_0 , \quad (2)$$

where k_{eff} is the effective stiffness of the cantilever with its mass center and deflection lumped to its tip, t the thickness, L_G the length of gate coupled to the cantilever, and ω_0 the angular frequency of the fundamental bending mode, with $k_{eff} = M_{eff}\omega_0^2$, and M_{eff} the effective mass of the cantilever. As soon as the cantilever tip contacts the drain (thus forming a beam clamped and supported at two ends), the voltage required for the cantilever to be pulled into the gate instantaneously increases to $V_{PI,G}$ (often noticeably higher than V_{on}). Therefore, for normal operations, V_G should be set or swept up to just slightly above V_{on}, and much lower than $V_{PI,G}$. Figure 1d & e show the estimation of V_{on} and t_s with dimensions of our present- and future-generation devices. Aggressive scaling toward very thin and short cantilevers ($w \times t \times L$~30nm×30nm×1μm or smaller) with very small gaps (≤30nm) can help in approaching V_{on} and t_s of modern logic circuits based on CMOS switches.

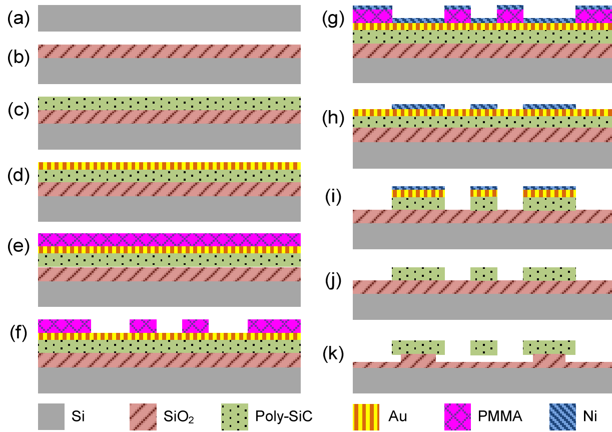

Figure 2: Nanofabrication process of SiC NEMS switches. (a) 4-inch Si wafer. (b) Thermal oxidation. (c) LPCVD deposition of poly-SiC. (d) Thermal evaporation of very thin Au layer. (e) Coating of PMMA. (f) EBL patterning of PMMA. (g) Evaporation of Ni masking layer. (h) Lift off. (i) Etching SiC by RIE. (j) Ni and PMMA residue removal. (k) Device release by vapor HF etching of SiO_2.

Figure 2 shows the detailed fabrication process of our SiC NEMS switches: starting from a 4-inch wafer of 500nm poly-SiC film grown by using LPCVD on 500nm SiO_2 on Si substrate, we use wafer-scale electron-beam lithography (EBL) to define all the patterns, and transfer patterns to SiC device layer by RIE, and finally release the devices by a high-yield vapor-HF etching of SiO_2.

MEASUREMENTS AND RESULTS

Figure 3a illustrates a schematic of the measurement setup for characterizing our poly-SiC NEMS switches. Two source measurement units (SMUs) are employed: one changes or sweeps the gate voltage V_G while monitoring gate (to source/ground) current I_G; the other provides a small constant voltage V_D (*e.g.*, often 100mV), while measuring the drain (to source/ground) current I_D.

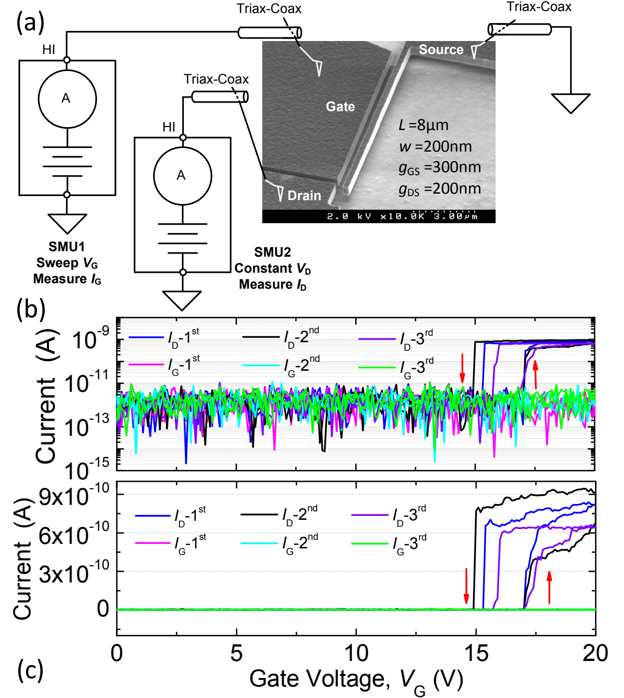

Figure 3: SiC NEMS switch measurement and basic I_D-V_G & I_G-V_G characteristics. (a) Scheme of measurement. (b) & (c) Measured characteristics showing abrupt switching on & off with hysteresis (see red arrows). I_D & I_G plotted in logarithmic scale (b) and linear scale (c), respectively.

SiC NEMS Switch Characteristics in Ambient Air

We first carefully explore the basic characteristics of individual switching events of the SiC NEMS switches. As discussed in the previous section, by sweeping V_G from 0 volt up to slightly above V_{on}, but well below $V_{PI,G}$ (both values are estimated by modeling with measured device dimensions), and then sweep V_G back to 0V, we record the I_D-V_G and I_G-V_G behavior in quasi-dc measurements.

Figure 3b & c show the current-voltage characteristics measured from the device shown in the inset of Fig. 3a, which has dimensions $L \times w \times t$ ≈8μm×200nm×500nm. The curves are from the first 3 times of repeatable switching, unambiguously demonstrating a few almost ideal features: (i) Sharply abrupt switching (of drain current I_D) between clearly defined 'Off' and 'On' states; (ii) Gate leakage (I_G) is zero (unmeasurably small) and does not appear to be varying with sweeping V_G; (iii) The 'Off' state $I_{D,Off}$ and I_G 'baseline' levels are not limited by the NEMS device, but by the triax-coax cable-probe assemblies and the applied measurement precision settings in each SMU; (iv) The switching has clear and intriguing hysteresis effects.

The particular NEMS device in Fig. 3a inset has shown a highly repeatable V_{on}≈17.0V and V_{off}≈15–15.3V, with small but noticeable fluctuations in V_{off}. The 'On' state drain current is $I_{D,On}$~0.6nA to ~1nA.

Figure 4 displays data from another device with same nominal dimensions $L \times w \times t$ ≈8μm×200nm×500nm, but slightly different gaps. This device demonstrates an 'On' voltage V_{on}≈17.9V, and switches off at V_{off}≈11.5V and

14.1V, for the first and second cycle, respectively. The 'On' state current $I_{D,On}$~150nA achieved in this device is much higher than that in the device shown in Fig. 3.

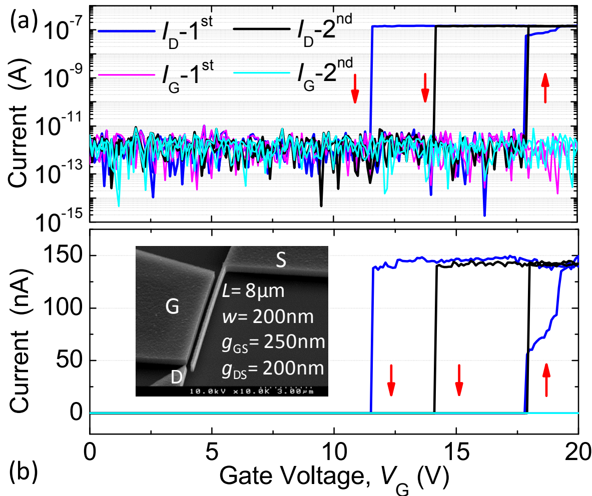

Figure 4: First two switching cycles with hysteresis, measured in another SiC NEMS switch, with currents in logarithmic scale (a) and linear scale (b), respectively. Inset of (b) is an SEM image of the actual device.

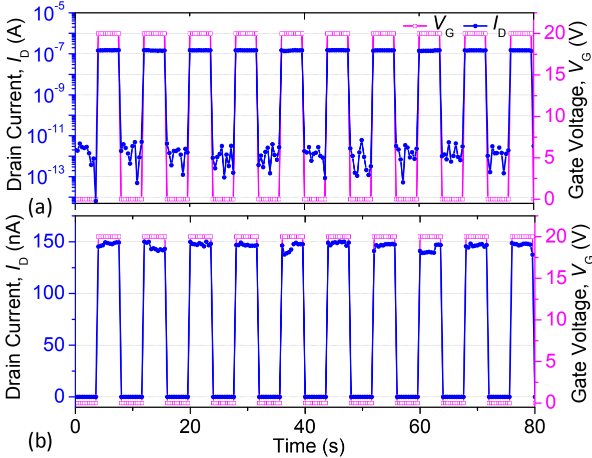

Figure 5: SiC NEMS switch operating multiple cycles over a minute following the applied gate voltage waveform, in (a) logarithmic scale and (b) linear scale, respectively.

Long Cycles of Hot Switching Recorded in Real Time

A critical metric, and a key challenge in NEMS switches, is the number of switching cycles that can be achieved by the device before failure (*i.e.*, the lifetime). In this work, for the first time in NEMS switches, we have carefully measured and *recorded the complete time evolution of all the switching events in real time*, as we switch on/off the devices throughout many cycles over days. Again we carefully choose V_G to be slightly above V_{on} but well below $V_{PI,G}$. Beyond estimation with modeling, we also quickly test and verify V_{on} for each device, via basic measurements discussed in Figs. 3 & 4. $V_{PI,G}$ can also be verified experimentally by sweeping V_G further up, but certainly with a risk of a failure mode of pulling the cantilever body into the gate.

We first demonstrate continuous repetitive switching by applying a periodic square-wave-like waveform for V_G, with peak voltage above the verified V_{on}. Figure 5 clearly demonstrates a train of such switching cycles (total 80sec): here the device (Fig. 4) has $V_{on}\approx17.9$V; the peak of the gate waveform is $V_{G,pk}$=20V; each cycle is 8sec, with a 4sec dwelling (NEMS in contact) time at the 'On' state.

We then perform long cycle tests on more devices, and attempt to explore their lifetime. One of such devices has a verified $V_{on}\approx15.8$V, and $I_{D,On}\approx10$nA. Figure 6 presents data obtained from this device, showing more than 14,000 cycles recorded in real time, over 7 consecutive days (still alive, preserved in vacuum for subsequent accelerated testing). In some hours each day, the device has been left idle, mimicking switching devices in practical situations.

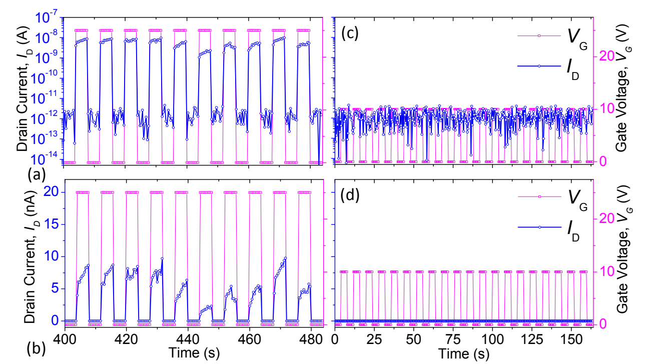

Figure 7: Representative switching cycles from the recorded long cycles. (a) & (b) Data selected randomly from day 1 (box 'A' in Fig. 6), I_D in logarithmic and linear scale, respectively. (c) & (d) Control tests show no NEMS switching when $V_{G,pk}$<V_{on} ('sub-threshold actuation').

Figure 7a & b show that in the first day the waveform with $V_{G,pk}$=25V (>V_{on}) nicely switches on/off the device. Figure 7c & d demonstrate a clear control experiment – when the waveform's peak voltage is below the threshold (switch-on) voltage, here $V_{G,pk}$=10V (<$V_{on}\approx15.8$V), I_D remains at the 'Off' state baseline level.

Figure 8 displays representative switching cycles and

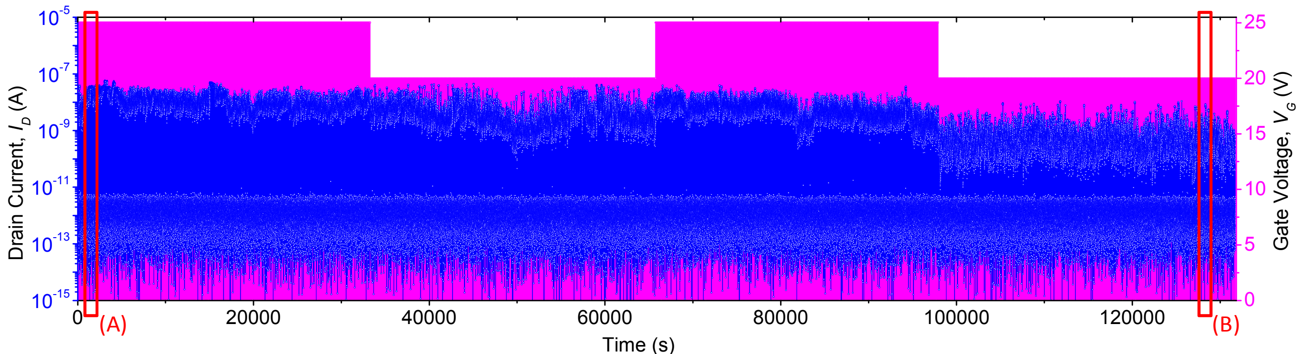

Figure 6: Over 14,000 switching cycles recorded in real time in 7 consecutive days (idle time not plotted). Blue is drain current I_D, magenta is actuation voltage waveform. Some data taken on day 1 and day 7 are marked in red boxes 'A' & 'B'.

hysteresis *I-V* curves from end of the long cycles in Fig. 6. This verifies that the device is still properly functional after the long cycles, with a noticeable decreasing average $I_{D,On}$, which suggests possible nanocontact degradation.

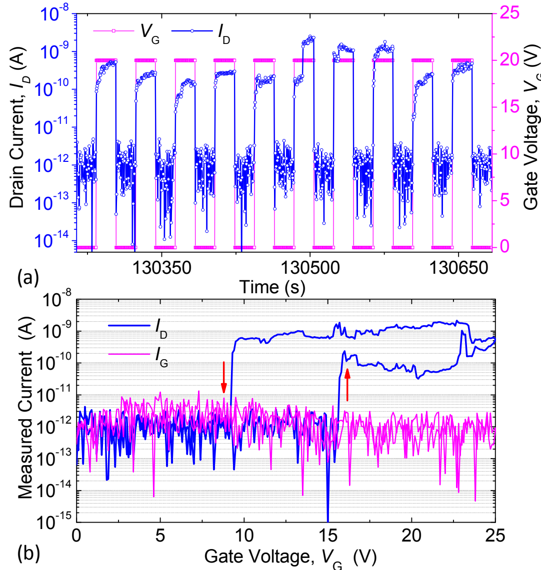

Figure 8: Switching cycles and hysteresis I-V curves at the end of long cycle testing shown in Fig. 6. (a) Switching cycles recorded near end of day 7 (box 'B' in Fig. 6). (b) Hysteresis I-V curves of the switch after >14,000 cycles.

High-Temperature (T≈500°C) Operations

Poly-SiC uniquely enables NEMS switching at high temperatures thanks to its outstanding thermal-mechanical properties. We have measured and recorded switching events at high temperature by directly heating the NEMS devices in air, up to carefully calibrated 500°C, using a specially designed high-temperature testing assembly. Figure 9 displays measured data from another 8μm-long, 200nm-wide device, showing clear switching at T≈500°C in air, with V_{on}≈10.2V and $I_{D,On}$≥100nA, comparable to those at T≈25°C. The off-state drain current $I_{D,Off}$ and gate leakage I_G are on the order of ~10^{-11}A to ~10^{-10}A.

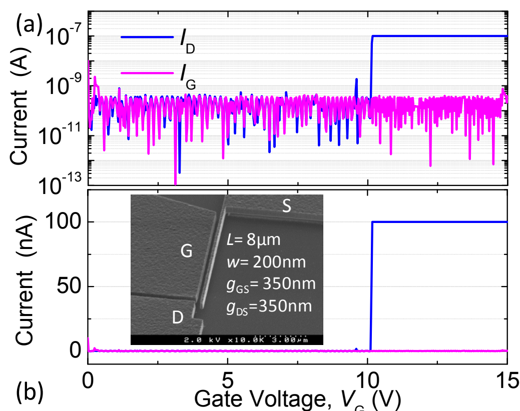

Figure 9: High temperature (T≈500°C) characteristics of a SiC NEMS switch, showing V_{on}≈10.2V with minimal gate and off-state drain leakage current, in (a) logarithmic and (b) linear scale, respectively. Inset is device SEM image.

CONCLUSIONS

With real-time recorded long cycles of repetitive 'hot' switching, we have demonstrated promising operations toward robust, long-lifetime poly-SiC NEMS switches that have very small dimensions and typical motional volume of only ~1μm³. Typical tested lifetime is at least 10^5–10^6 cycles without failure (>10^6 traces too dense to plot). We benchmark device performance in Fig. 10, along with other genuinely nanoscale electromechanical switches recently reported. In comparison, our SiC NEMS switches have the highest recorded numbers of switching cycles. Moreover, these long-cycle devices are still alive, and are currently under study in challenging high-speed measurements at ~nA–μA levels to properly measure their ultimate lifetime.

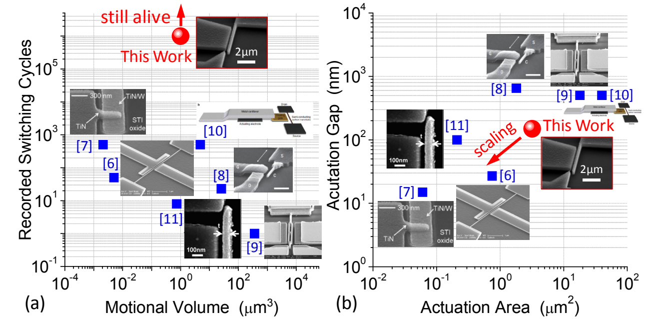

Figure 10: Benchmarking performance and specs of our SiC NEMS with other NEMS switches recently reported. (a) Recorded number of switching cycles versus device motional volume. (b) Actuation gap versus actuation area.

ACKNOWLEDGEMENTS

The authors are grateful to the support from DARPA (NEMS Program, D11AP00292) & NSF (CCF-1116102).

REFERENCES

[1] M. L. Roukes, "Mechanical computation, redux?" in *Tech. Digest of IEDM,* San Francisco, CA, Dec. 13-15, 2004, pp. 539-542.

[2] V. Pott, *et al.*, "Mechanical computing redux: relays for integrated circuit applications", *Proc. IEEE*, vol. 98, no. 12, pp. 2076-2094, Dec. 2010.

[3] H. Kam, *et al.*, "Design and reliability of a micro-relay technology for zero-standby-power…", in *Tech. Digest of IEDM*, Baltimore, MD, Dec. 7-9, 2009, pp. 809-812.

[4] Y. Lin, *et al.*, "A resonance dynamical approach to faster, more reliable…", in *Proc. IEEE Int. Freq. Contr. Symp. (IFCS)*, Honolulu, HI, May 19-21, 2008, pp. 640-645.

[5] N. Sinha, *et al.*, "Body-biased complementary logic implemented using AlN…", *J. Microelectromech. Syst.*, vol. 21, no. 2, pp. 484-496, Apr. 2012.

[6] X. L. Feng, *et al.*, "Low voltage nanoelectromechanical switches based on silicon carbide nanowires", *Nano Letters,* vol. 10, no. 8, pp. 2891-2896, Aug. 2010.

[7] W. W. Jang, *et al.*, "Fabrication and characterization of a nanoelectromechanical switch with 15-nm-thick…", *Appl. Phys. Lett.*, vol. 92, art. no. 103110, Mar. 2008.

[8] Y. Hayamizu, *et al.*, "Integrated three-dimensional microelectromechanical devices from processable carbon …", *Nat. Nanotech.*, vol. 3, no. 5, pp. 289-294, May 2008.

[9] R. Parsa, *et al.*, "Nanoelectromechanical relays with decoupled electrode and suspension", in *Proc. Int. IEEE MEMS Conf.*, Jan. 23-27, 2011, pp. 1361-1364.

[10] S. W. Lee, *et al.*, "A fast and low-power…", *Nat. Commun.*, vol. 2, art. no. 220, Mar. 2011.

[11] S. Chong, *et al.*, "Integration of nanoelectromechanical relays with silicon nMOS", *IEEE Trans. Elect. Dev.*, vol. 59, no. 1, pp. 255-258, Jan. 2012.